Nonadiabatic quantum molecular dynamics with hopping. I. General formalism and case study

M. Fischer, J. Handt, and R. Schmidt*
Institut für Theoretische Physik, Technische Universität Dresden, D-01062 Dresden, Germany
(Received 30 April 2014; published 29 July 2014)

An extension of the nonadiabatic quantum molecular dynamics approach is presented to account for electron-nuclear correlations in the dynamics of atomic many-body systems. The method combines electron dynamics described within time-dependent density-functional or Hartree-Fock theory with trajectory-surface-hopping dynamics for the nuclei, allowing us to take into account explicitly a possible external laser field. As a case study, a model system of $H^+ + H$ collisions is considered where full quantum-mechanical calculations are available for comparison. For this benchmark system the extended surface-hopping scheme exactly reproduces the full quantum results. Future applications are briefly outlined.

DOI: 10.1103/PhysRevA.90.012525 PACS number(s): 31.15.xv, 31.15.ee, 36.40.−c, 34.50.Gb

I. INTRODUCTION

During the last decades, the investigation of nonadiabatic phenomena in finite atomic many-body systems has become a vast research field in atomic and molecular physics, quantum chemistry, and related areas, e.g., atomic cluster physics. Nonadiabatic processes are characterized by collision- or light-induced electronic excitations coupled to the nuclear dynamics in molecules or clusters [1].

Triggered by the availability of powerful laser sources working in the femtosecond regime [2,3], experiments have been able to uncover a variety of fascinating (nonadiabatic) phenomena, among them above-threshold dissociation [4], charge-resonance-enhanced ionization [5], molecular alignment [6], ultrafast internal conversion [7], and Coulomb explosion [8]. Present-day pump-probe techniques allow one to follow the nuclear dynamics in laser-induced processes in real time [9]. In addition, refined scattering experiments have delivered detailed insight into reaction mechanisms in ion-molecule or ion-cluster collisions such as electronic and vibrational excitation, ionization, charge transfer, and fragmentation [10–12].

The theoretical description of nonadiabatic processes is a challenging task, as in principle the solution of the time-dependent Schrödinger equation (TDSE) for the whole atomic many-body system is required for this purpose. Such a full-dimensional quantum-mechanical description is, at present, limited to nature's smallest molecule H_2^+ (or D_2^+) exposed to a laser field in which ionization can be neglected [13,14]. For the neutral hydrogen molecule, H_2, an exact quantum-mechanical solution has been obtained, so far only with a restricted number of degrees of freedom (DOF), e.g., using the fixed-nuclei approximation [15–17] or restricting the molecule to be aligned along the laser polarization axis [18,19]. Evidently, for larger systems, approximations are inevitable.

The full quantum-mechanical solution can be circumvented by means of a mixed classical-quantum description, i.e., coupling (not necessarily pure) classical molecular dynamics (MD) for the nuclei to the electronic system described entirely quantum mechanically. The basic problem of such a scheme concerns the way the coupling between the classical and quantum subsystems is treated [20].

The most straightforward way to realize this coupling results naturally in the mean-field approximation for the nuclear dynamics [21–24], often called the Ehrenfest method [20,25–27]. In this approximation, the nuclei propagate purely classically on an effective time-dependent potential-energy surface, which is an average over the electronic subsystem. The Ehrenfest method is therefore appropriate for describing situations where the quantum nature of the nuclear motion is negligible (e.g., in high-energy atom-cluster collisions [28,29]) and/or calculating *mean* observables which are not largely affected by quantum effects of the nuclear dynamics (e.g., the mean absorbed energy within a molecule exposed to an intense laser field [30]). In other words, the Ehrenfest dynamics fails to treat processes which are dominated by the wave-packet dynamics of the nuclei (e.g., in chemical reactions [31]) and/or to obtain *differential* experimental quantities which are *a priori* determined by the inherent quantum nature of the nuclei (e.g., the kinetic-energy release of the products resulting from laser- or collision-induced fragmentation of a molecule [11]).

To overcome the limitations of the mean-field or Ehrenfest dynamics represents a challenging and ongoing field of the time-dependent theory of finite atomic many-body systems [20]. Thereby, the ultimate goal consists of the development of a theory (in any case still approximate) which describes self-consistently the coupled electron-nuclear dynamics on full quantum-mechanical footings. To realize this, very different attempts have been proposed so far. They include a rigorous reformulation of the TDSE by means of a two-component (nuclei and electrons) time-dependent density-functional theory (TD-DFT) [32], an *ab initio* multiple-spawning MD [33], and a moment expansion of the density matrix in the exact Ehrenfest equations [34], as well as a number of *ab initio* MD methods [35–38] based on TD-DFT [39] and Tully's surface-hopping mechanism [40] to include electron-nuclear correlations.

The so-called nonadiabatic quantum molecular dynamics (NA-QMD) method developed by our group [21,22,41,42] describes self-consistently electronic excitations (in terms of TD-DFT in the local basis expansion) and classical nuclear motion (in the sense of the Ehrenfest dynamics) in finite atomic many-body systems. With this universal theory, a large variety

*Ruediger.Schmidt@tu-dresden.de

of very different collision- and laser-induced nonadiabatic processes has been investigated so far (for an overview see [43]). For collisions this concerns, among other things, the "stopping power" in metallic clusters [28] and fullerenes [29], the charge transfer in ion-cluster collisions [44–46] and highly charged ion-molecule collisions [47], the dissociation mechanisms in collisions between ions and molecules [11], and the reaction mechanisms in collisional systems as large as fullerene-fullerene reactions [48]. Concerning laser-induced nonadiabatic phenomena, the NA-QMD method was used in the past to study, for example, the isomerization of small organic molecules in femtosecond laser pulses [49,50], the excitation of the giant breathing mode in fullerenes [30], the orientation dependence of energy absorption and relaxation dynamics of C_{60} in femtosecond laser pulses [51], and the alignment, dissociation, and ionization of the molecular benchmark system H_2^+ and its mother molecule, H_2, exposed to intense laser fields [52,53]. Thereby, the first "complete" study of a molecular system exposed to an intense laser field (i.e., including *all* electronic and nuclear DOF as well as dissociation and ionization) could be achieved [54].

This broad range of applications could be realized by systematically extending the theory associated with a permanent improvement or extension of the local basis expansion as the heart of its technical implementation. So the original approximate (not *ab initio*) version [21] was restricted to conservative systems (i.e., collisional problems) and used Slater-type functions to represent the atomic orbitals (AOs) as basis functions. The following *ab initio* version [22] made it possible to include explicitly external laser fields and used standard quantum-chemical basis sets [55–57] to represent the AOs. Later, it was generalized to describe also ionization [41] in a *local basis expansion* involving additional gridlike Gaussian basis functions. A systematic estimate of the basis-set expansion error has been given in [42].

In principle, the only physical approximation of the present version of the NA-QMD method consists of the purely classical, i.e., mean-field or Ehrenfest, treatment of the nuclei. With the present series of papers, we develop in this work (Paper I of this series) and apply in Refs. [61,62] an extended formalism of the NA-QMD. It includes quantum effects in the nuclear dynamics by coupling self-consistently the nonadiabatic equations of motion (EOM) for the electrons with a trajectory-surface-hopping scheme in the adiabatic framework for the nuclei, called nonadiabatic quantum molecular dynamics with hopping (NA-QMD-H).

The original idea for such an approach, i.e., coupling surface hopping with TD-DFT, was first discussed in [35]. Here, in Sec. II, we develop in detail the NA-QMD-H formalism and compare it with other existing *ab initio* MD methods based on TD-DFT and the surface-hopping technique [36–38]. Special attention is drawn to a clear presentation of different basis expansions or transformations of the single-particle wave functions, i.e., time-dependent Kohn-Sham (KS) or Hartree-Fock (HF) orbitals, needed in the NA-QMD-H formalism. We also discuss how the adiabatic limiting case, the so-called quantum molecular dynamics [58], i.e., classical MD combined with time-independent DFT for the electronic ground state, can be derived from the EOM of the NA-QMD and NA-QMD-H formalisms. The broad range of adiabatic processes, in which electronic transitions are negligible (e.g., collisions with purely rovibrational excitations [59] or low-intensity infrared laser excitations [60]), can be described in the QMD approximation, which requires significantly less computational effort compared to any nonadiabatic theory (for a review of QMD see, e.g., [58]).

Finally, in Sec. III we illustrate the relevance of electron-nuclear correlations in atomic collisions, intentionally using the simplest possible collision model for the $H^+ + H$ system. Different measurable quantities are calculated within NA-QMD and NA-QMD-H and compared with exact quantum-mechanical calculations available for this benchmark system.

Future applications in many-electron systems are briefly discussed in Sec. IV and will be outlined in papers II and III of this series [61,62].

II. THEORY

In this section we briefly review the NA-QMD method (Sec. II A), develop its extended NA-QMD-H version (Sec. II B), and discuss the adiabatic QMD limit of both approaches (Sec. II C). The molecular system is first and foremost divided into a quantum subsystem of N_e electrons described by a wave function $\Psi(\mathbf{r}_1\sigma_1,\ldots,\mathbf{r}_{N_e}\sigma_{N_e})$ and a classical subsystem with N_i classical particles (ions or nuclei) described by the trajectories $\mathbf{R}(t) = \{\mathbf{R}_1(t)\cdots\mathbf{R}_{N_i}(t)\}$. Atomic units are used throughout this section.

A. Nonadiabatic quantum molecular dynamics

The NA-QMD method in its present form represents a self-consistent description of electron dynamics within TD-DFT or Hartree-Fock theory (TD-HF) in the *basis expansion* with classical dynamics for the nuclei. Here, we rederive the respective EOM, slightly extended compared to those in [22], i.e., including the TD-HF version of the theory.

1. General formalism

The total action of the mixed quantum-classical molecular system

$$A = A_{\mathrm{cl}} + A_{\mathrm{qm}} \tag{1}$$

consists of a classical part,

$$A_{\mathrm{cl}} = \int_{t_0}^{t_1}\left\{\sum_{A=1}^{N_i}\frac{M_A}{2}\dot{\mathbf{R}}_A^2 - U(\mathbf{R},t)\right\}dt, \tag{2}$$

and a quantum-mechanical part [63],

$$A_{\mathrm{qm}} = \int_{t_0}^{t_1}\langle\Psi|i\frac{\partial}{\partial t} - \mathcal{H}|\Psi\rangle dt. \tag{3}$$

The classical action (2) contains the interaction potential

$$U(\mathbf{R},t) = \sum_{A<B}^{N_i}\frac{Z_A Z_B}{|\mathbf{R}_A - \mathbf{R}_B|} - \sum_{A=1}^{N_i} Z_A\mathbf{R}_A\cdot\mathbf{E}(t), \tag{4}$$

which describes the Coulomb repulsion of the ions (with masses M_A and charges Z_A) as well as the interaction of the ions with a possible external laser electric field $\mathbf{E}(t)$.

The quantum-mechanical action (3) contains the many-electron Hamiltonian

$$\mathcal{H} = -\sum_{i=1}^{N_e} \frac{\nabla_{\mathbf{r}_i}^2}{2} - \sum_{i=1}^{N_e}\sum_{A=1}^{N_i} \frac{Z_A}{|\mathbf{r}_i - \mathbf{R}_A|} + \sum_{i<j}^{N_e} \frac{1}{|\mathbf{r}_i - \mathbf{r}_j|} + \sum_{i=1}^{N_e} \mathbf{r}_i \cdot \mathbf{E}(t) \tag{5}$$

as well as the many-electron wave function Ψ, which is represented by a Slater determinant in the framework of TD-DFT or TD-HF. The latter fact allows us to rewrite (3) as

$$A_{\mathrm{qm}} = \int_{t_0}^{t_1} \int \sum_{\sigma=\uparrow\downarrow} \sum_{j=1}^{N_e^\sigma} \Psi^{j\sigma *}(\mathbf{r},t)\left[i\frac{\partial}{\partial t} + \frac{\nabla_{\mathbf{r}}^2}{2}\right]\Psi^{j\sigma}(\mathbf{r},t) d^3r dt - A_{\mathrm{pot}}\,, \tag{6}$$

where $\Psi^{j\sigma}(\mathbf{r},t)$ are the time-dependent single-particle functions j for spin $\sigma(\sigma = \uparrow,\downarrow)$ and $\mathbf{r}$ denotes the one-electron coordinate. The potential term in (6) reads

$$A_{\mathrm{pot}} = \int_{t_0}^{t_1} \int \rho(\mathbf{r},t)\left[V(\mathbf{r},\mathbf{R},t) + \frac{1}{2}\int \frac{\rho(\mathbf{r}',t)}{|\mathbf{r}-\mathbf{r}'|} d^3r'\right] d^3r dt + A_{\mathrm{xc}}[\rho^\uparrow,\rho^\downarrow] \tag{7}$$

and is a functional of the electronic (single-particle) spin densities ρ^σ given by

$$\rho^\sigma(\mathbf{r},t) = \sum_{j=1}^{N_e^\sigma} \Psi^{j\sigma *}(\mathbf{r},t)\Psi^{j\sigma}(\mathbf{r},t) \tag{8}$$

and the total electronic (single-particle) density given by the sum of the two spin contributions,

$$\rho(\mathbf{r},t) = \sum_{\sigma=\uparrow,\downarrow} \rho^\sigma(\mathbf{r},t). \tag{9}$$

The external potential $V(\mathbf{r},\mathbf{R},t)$ in (7) includes the electron-nuclear attraction and a possible electron-laser interaction potential (in dipole approximation with length gauge),

$$V(\mathbf{r},\mathbf{R},t) = -\sum_{A=1}^{N_i} \frac{Z_A}{|\mathbf{R}_A - \mathbf{r}|} + \mathbf{r}\cdot\mathbf{E}(t), \tag{10}$$

and A_{xc} is the exchange correlation term which, in the spirit of DFT and HF, can be assumed to be a functional of the single-particle spin density.

The equations of motion for the time-dependent Kohn-Sham or Hartree-Fock functions $\Psi^{j\sigma}(\mathbf{r},t)$ and the classical trajectories $\mathbf{R}_A(t)$ follow from the variational principle applied to the total action (1). By variation with respect to the single-particle functions one derives the time-dependent equations

$$i\frac{\partial}{\partial t}\Psi^{j\sigma}(\mathbf{r},t) = \left[-\frac{\nabla_{\mathbf{r}}^2}{2} + V_{\mathrm{s}}^\sigma(\mathbf{r},\mathbf{R},t)\right]\Psi^{j\sigma}(\mathbf{r},t), \tag{11}$$

with the effective single-particle potential

$$V_{\mathrm{s}}^\sigma(\mathbf{r},\mathbf{R},t) = V(\mathbf{r},\mathbf{R},t) + \int \frac{\rho(\mathbf{r}',t)}{|\mathbf{r}-\mathbf{r}'|} d^3r' + \frac{\delta A_{\mathrm{xc}}[\rho^\uparrow,\rho^\downarrow]}{\delta\rho^\sigma(\mathbf{r},t)}. \tag{12}$$

The exchange-correlation part is unknown in general and thus has to be approximated in practical calculations, e.g., with the adiabatic local spin-density approximation (ALSDA) [64,65] or with the exact nonlocal Hartree-Fock exchange (for details see [66]). Thus, Eq. (11) represent either the time-dependent KS or HF equations, and the operator on the right-hand side of (11) is the KS or HF Hamiltonian

$$H^\sigma = -\frac{\nabla_{\mathbf{r}}^2}{2} + V_{\mathrm{s}}^\sigma(\mathbf{r},\mathbf{R},t). \tag{13}$$

The classical equations of motion result from variation with respect to the classical trajectories $\mathbf{R}_A(t)$ as

$$M_A\ddot{\mathbf{R}}_A = -\frac{\partial U}{\partial \mathbf{R}_A} + \int \rho(\mathbf{r},t)\frac{\partial V(\mathbf{r},\mathbf{R},t)}{\partial \mathbf{R}_A} d^3r \tag{14}$$

in both cases.

In principle, the coupled EOM (11) and (14) have to be solved simultaneously with appropriate initial conditions. However, the direct solution of (11) and (14) on a numerical grid would restrict the range of applications of the theory drastically; for example, it would be impossible to consider molecular collisions, laser-induced ionization, or fragmentation owing to the unrealizable numerical effort. Therefore, the core part of the NA-QMD method is a *local basis expansion* of the single-particle orbitals, as outlined in the next section.

2. *Local atomic basis expansion and effective potential-energy surface*

In order to feasibly solve the coupled EOM (11) and (14), the single-particle functions are expanded into a set of local atomic basis functions ϕ_α as

$$\Psi^{j\sigma}(\mathbf{r},t) = \sum_\alpha a_\alpha^{j\sigma}(t)\phi_\alpha\left(\mathbf{r} - \mathbf{R}_{A_\alpha}\right). \tag{15}$$

The time-dependent electronic density (9) in the local basis reads

$$\rho(\mathbf{r},t) = \sum_{\sigma=\uparrow\downarrow}\sum_{j=1}^{N_e^\sigma}\sum_{\alpha\beta} a_\alpha^{j\sigma *}(t)a_\beta^{j\sigma}(t) \times \phi_\alpha^*\left(\mathbf{r} - \mathbf{R}_{A_\alpha}\right)\phi_\beta\left(\mathbf{r} - \mathbf{R}_{A_\beta}\right). \tag{16}$$

It is convenient to define a variety of matrix elements corresponding to this basis expansion:
(i) the overlap matrix

$$S_{\alpha\beta} = \langle\phi_\alpha|\phi_\beta\rangle, \tag{17}$$

(ii) the (Kohn-Sham) Hamilton matrix

$$H_{\alpha\beta}^\sigma = \langle\phi_\alpha|H^\sigma|\phi_\beta\rangle, \tag{18}$$

and (iii) the nonadiabatic coupling matrix

$$B_{\alpha\beta} = \left\langle\phi_\alpha\middle|\frac{d}{dt}\phi_\beta\right\rangle, \tag{19}$$

as well as (iv) the vector matrices

$$\mathbf{B}_{\alpha\beta}^A = \left\langle\phi_\alpha\middle|\frac{\partial}{\partial\mathbf{R}_A}\phi_\beta\right\rangle, \tag{20}$$

$$\mathbf{B}_{\alpha\beta}^{A+} = \left\langle\frac{\partial}{\partial\mathbf{R}_A}\phi_\alpha\middle|\phi_\beta\right\rangle, \tag{21}$$

$$\mathbf{C}^{A}_{\alpha\beta} = \left\langle \frac{d}{dt}\phi_\alpha \middle| \frac{\partial}{\partial \mathbf{R}_A}\phi_\beta \right\rangle, \tag{22}$$

$$\mathbf{C}^{A+}_{\alpha\beta} = \left\langle \frac{\partial}{\partial \mathbf{R}_A}\phi_\alpha \middle| \frac{d}{dt}\phi_\beta \right\rangle \tag{23}$$

and (v) the combined force matrix

$$\mathbf{K}^{A\sigma}_{\alpha\beta} = \sum_{\gamma\delta}\left(\mathbf{B}^{A+}_{\alpha\gamma} S^{-1}_{\gamma\delta} H^{\sigma}_{\delta\beta} + H^{\sigma}_{\alpha\gamma} S^{-1}_{\gamma\delta}\mathbf{B}^{A}_{\delta\beta}\right) + i\left[\mathbf{C}^{A+}_{\alpha\beta} - \mathbf{C}^{A}_{\alpha\beta} + \sum_{\gamma\delta}\left(B^{+}_{\alpha\gamma} S^{-1}_{\gamma\delta}\mathbf{B}^{A}_{\delta\beta} - \mathbf{B}^{A+}_{\alpha\gamma} S^{-1}_{\gamma\delta} B_{\delta\beta}\right)\right]. \tag{24}$$

The first term in (24) contains the nonadiabatic couplings $\mathbf{B}^{A}_{\alpha\beta}$, whereas the second term gives rise to the force corrections due to the finiteness of the basis set (see below). Due to the dependence of the KS or HF Hamiltonian (13) on the electronic density (16), the Hamilton matrix (18) and the vector matrix (24) depend implicitly on the time-dependent expansion coefficients $a^{j\sigma}_{\alpha}(t)$.

The total energy $E_{\mathrm{tot}}(t)$ of the system reads [22]

$$E_{\mathrm{tot}}(t) = \sum_{A=1}^{N_{\mathrm{i}}} \frac{M_A}{2}\dot{\mathbf{R}}^2_A + E(t). \tag{25}$$

The second term $E(t)$ in (25) defines the *effective* time-dependent potential-energy surface for the nuclear dynamics and is given by

$$E(t) = \sum_{\sigma=\uparrow\downarrow}\sum_{j=1}^{N^{\sigma}_{\mathrm{e}}}\sum_{\alpha\beta} a^{j\sigma *}_{\alpha}(t)\left[T_{\alpha\beta} + V_{\alpha\beta} + \frac{1}{2}\sum_{\sigma'=\uparrow\downarrow}\sum_{j'=1}^{N^{\sigma'}_{\mathrm{e}}}\sum_{\gamma\delta} Q_{\alpha\beta\gamma\delta} a^{j'\sigma' *}_{\gamma}(t) a^{j'\sigma'}_{\delta}(t)\right] a^{j\sigma}_{\beta}(t) + E_{\mathrm{xc}}[\rho](t) + U(\mathbf{R},t), \tag{26}$$

with the matrix elements

$$T_{\alpha\beta} = \langle\phi_\alpha| -\frac{\nabla^2_{\mathbf{r}}}{2}|\phi_\beta\rangle, \tag{27}$$

$$V_{\alpha\beta} = \langle\phi_\alpha| V(\mathbf{r},\mathbf{R},t)|\phi_\beta\rangle, \tag{28}$$

$$Q_{\alpha\beta\gamma\delta} = \int d^3r \int d^3r' \phi^*_\alpha(\mathbf{r}-\mathbf{R}_{A_\alpha})\phi_\beta(\mathbf{r}-\mathbf{R}_{A_\beta}) \times \frac{1}{|\mathbf{r}-\mathbf{r}'|}\phi^*_\gamma(\mathbf{r}'-\mathbf{R}_{A_\gamma})\phi_\delta(\mathbf{r}'-\mathbf{R}_{A_\delta}), \tag{29}$$

the exchange correlation energy $E_{\mathrm{xc}}[\rho](t)$, and the nuclear potential $U(\mathbf{R},t)$ given in Eq. (4).

3. *Equations of motion in the basis expansion*

With the basis expansion (15) and the corresponding matrix elements defined above the time-dependent Kohn-Sham or Hartree-Fock equations (11) follow from the variation of the total action with respect to the time-dependent expansion coefficients as [22]

$$\dot{a}^{j\sigma}_{\alpha}(t) = -\sum_{\beta\gamma} S^{-1}_{\alpha\beta}\left(i H^{\sigma}_{\beta\gamma} + B_{\beta\gamma}\right) a^{j\sigma}_{\gamma}(t), \tag{30}$$

and analogously, the classical equations of motion (14) are derived by the variation of the total action with respect to the classical trajectories as

$$M_A\ddot{\mathbf{R}}_A = -\frac{\partial E(t)}{\partial \mathbf{R}_A} + \sum_{\sigma=\uparrow\downarrow}\sum_{j=1}^{N^{\sigma}_{\mathrm{e}}}\sum_{\alpha\beta} a^{j\sigma *}_{\alpha}(t)\mathbf{K}^{A\sigma}_{\alpha\beta} a^{j\sigma}_{\beta}(t). \tag{31}$$

This set of equations has to be solved self-consistently, as the matrix elements in (30) depend on the classical coordinates and the force on the nuclei in (31) depends on the quantum-mechanical expansion coefficients. We note that the matrix element $\mathbf{K}^{A\sigma}_{\alpha\beta}$ [see (24)] contains the nonadiabatic couplings and a velocity-dependent correction term that appears in the forces due to the finiteness of the local basis set. A transparent interpretation of these complicated force corrections, resulting from the incompleteness of the basis $\{\phi_\alpha\}$, has been given in [22].

As can be explicitly seen from the classical equations of motion (31) or even more directly in Eq. (14), the NA-QMD method represents a *mean-field* or *Ehrenfest* approach, as the force is given by an average over the quantum-mechanical subsystem. Nuclear dynamics proceeds fully classically on one *effective* explicitly time-dependent potential-energy surface, and thus, electron-nuclear correlations are not taken into account.

In order to approximately account for quantum effects in the nuclear dynamics, the formalism must be basically extended, as described in the next section.

B. Nonadiabatic quantum molecular dynamics with trajectory surface hopping

In the following, we go beyond the mean-field version of NA-QMD presented in Sec. II A and extend the theory in order to approximately take into account electron-nuclear correlations by means of a trajectory-surface-hopping scheme. The basic idea of Tully's surface-hopping approach consists of approximating the nuclear wave-packet dynamics by an ensemble of classical trajectories moving on randomly chosen and suddenly changing potential-energy surfaces. The transition (hopping) probabilities between these surfaces are determined by the nonadiabatic couplings between the corresponding states. In doing so, the same initial state leads to an ensemble of different trajectories representing a classically sampled wave packet, disregarding, however, all interference effects.

In the following, for simplicity, we will exclusively make use of the terminology of DFT and call, e.g., $\Psi^{j\sigma}(\mathbf{r},t)$ KS functions. The TD-HF version of the theory follows automatically from the consideration presented in the previous section.

1. *Adiabatic many-particle states and energy surfaces*

In this section, we define the adiabatic many-particle states and corresponding (excited) potential-energy surfaces on

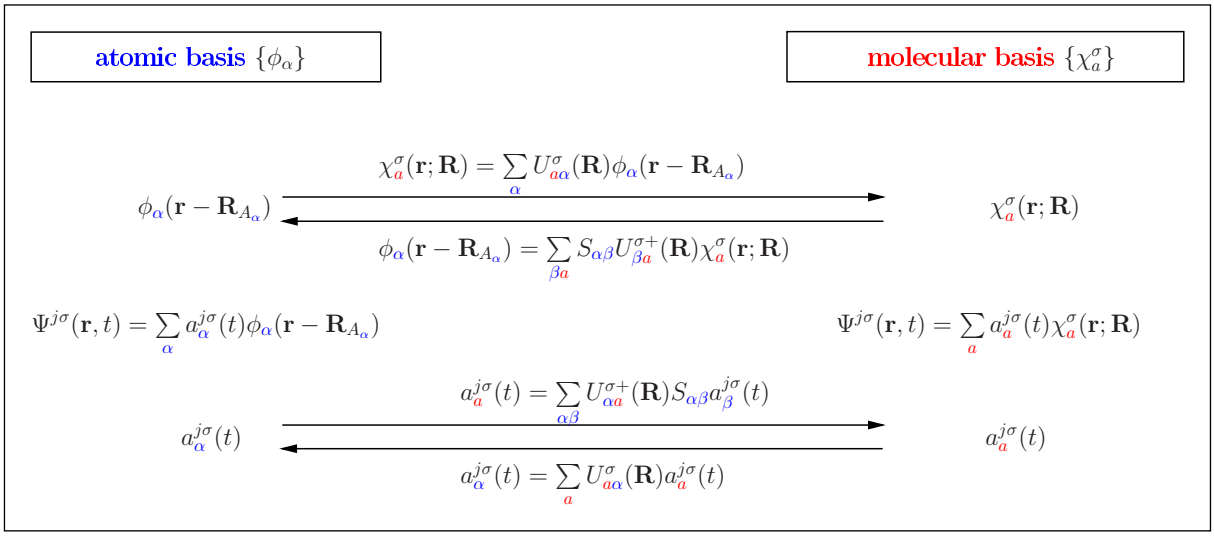

FIG. 1. (Color online) Overview of notations, transformations, and representations of single-particle functions belonging (left) to the atomic basis $\{\phi_\alpha(\mathbf{r}-\mathbf{R}_{A_\alpha})\}$ and (right) to the molecular basis $\{\chi_a^\sigma(\mathbf{r};\mathbf{R})\}$. Throughout the paper, the Greek indices $\alpha,\beta,\gamma,\delta$ correspond to the atomic basis, whereas the Latin indices a,b belong to the molecular basis. First row: Transformations between both basis functions. Second row: Expansions of the time-dependent KS functions in both basis sets. Third row: Transformations between the time-dependent expansion coefficients.

which the nuclear propagation will proceed in the NA-QMD-H approach.

To this end, we start from the ordinary, field-free, time-independent ground-state KS equations for a given (fixed) nuclear configuration $\mathbf{R}$,

$$\left[-\frac{\nabla_{\mathbf{r}}^2}{2} + V_{\mathrm{gs,s}}^\sigma(\mathbf{r},\mathbf{R})\right]\chi_a^\sigma(\mathbf{r};\mathbf{R}) = \epsilon_a^\sigma(\mathbf{R})\chi_a^\sigma(\mathbf{r};\mathbf{R}), \tag{32}$$

where $\chi_a^\sigma(\mathbf{r};\mathbf{R})$ and $\epsilon_a^\sigma(\mathbf{R})$ are the single-particle KS functions and corresponding single-particle energies. The effective single-particle potential $V_{\mathrm{gs,s}}^\sigma(\mathbf{r},\mathbf{R})$ is given by

$$V_{\mathrm{gs,s}}^\sigma(\mathbf{r},\mathbf{R}) = V(\mathbf{r},\mathbf{R}) + \int \frac{\rho_{\mathrm{gs}}(\mathbf{r}')}{|\mathbf{r}-\mathbf{r}'|}d^3r' + \frac{\delta A_{\mathrm{xc}}[\rho_{\mathrm{gs}}^\uparrow,\rho_{\mathrm{gs}}^\downarrow]}{\delta\rho_{\mathrm{gs}}^\sigma(\mathbf{r})}. \tag{33}$$

It contains the *field-free* external potential $V(\mathbf{r},\mathbf{R})$, i.e., the electron-nuclear attraction [Eq. (10) without the laser field], and it is a functional of the ground-state electronic density

$$\rho_{\mathrm{gs}}(\mathbf{r}) = \sum_{\sigma=\uparrow\downarrow}\sum_{a=1}^{N_{\mathrm{e}}^\sigma}\chi_a^{\sigma*}(\mathbf{r};\mathbf{R})\chi_a^\sigma(\mathbf{r};\mathbf{R}) \tag{34}$$

and defines the ground-state Kohn-Sham Hamiltonian

$$H_{\mathrm{gs}}^\sigma = -\frac{\nabla_{\mathbf{r}}^2}{2} + V_{\mathrm{gs,s}}^\sigma(\mathbf{r},\mathbf{R}). \tag{35}$$

The sum in (34) belongs to the lowest occupied states.

Now, in order to solve the eigenvalue problem (32) we expand the single-particle states $\chi_a^\sigma(\mathbf{r};\mathbf{R})$ in the same local basis set $\{\phi_\alpha\}$ as in the time-dependent NA-QMD case (15),

$$\chi_a^\sigma(\mathbf{r};\mathbf{R}) = \sum_\alpha U_{a\alpha}^\sigma(\mathbf{R})\phi_\alpha\big(\mathbf{r}-\mathbf{R}_{A_\alpha}\big), \tag{36}$$

and thus, the KS equations (32) are converted into their local basis-set representation,

$$\sum_\beta\big[H_{\mathrm{gs},\alpha\beta}^\sigma(\mathbf{R}) - \epsilon_a^\sigma(\mathbf{R})S_{\alpha\beta}(\mathbf{R})\big]U_{a\beta}^\sigma(\mathbf{R}) = 0, \tag{37}$$

with $H_{\mathrm{gs},\alpha\beta}^\sigma = \langle\phi_\alpha|H_{\mathrm{gs}}^\sigma|\phi_\beta\rangle$ being the ground-state Hamilton matrix.

Note that in Eqs. (36) and (37) and consistently in all following formulas, the Greek indices α,β belong to the local atomic basis set $\{\phi_\alpha\}$, whereas the Latin index a belongs to the adiabatic molecular basis $\{\chi_a^\sigma\}$. For a concise overview, we have summarized in Fig. 1 the relevant notations of and transformations between both basis sets, including those of the time-dependent case, which is needed afterwards.

The eigenvalue problem (37) has to be solved iteratively, as the Hamiltonian (35) depends on the ground-state density (34) and the expansion coefficients $U_{a\beta}^\sigma(\mathbf{R})$. Note that this Hamiltonian differs basically from that used in the time-dependent Kohn-Sham equations (11) and (30). Here, we consider the field-free ground state at a fixed classical configuration $\mathbf{R}$, and thus, the energies $\epsilon_a^\sigma(\mathbf{R})$ represent (field-free) single-particle energies in the (ground-state) Kohn-Sham framework for the respective spin.

The many-electron ground state corresponds to a single Slater determinant in the KS formalism, constructed from the occupied single-particle states in (34). Excited states can be calculated from all adiabatic basis functions $\{\chi_a^\sigma\}$ on different levels of approximation [36–38]. Here we use single-particle excitations in the KS Slater determinants, which have been shown to be well-defined approximations for the real excitation energies in many cases [67,68] (see also the critical discussion below).

Therefore, the many-electron states corresponding to the adiabatic single-particle states χ_a^σ are given by adiabatic Slater

determinants for spin σ,

$$\Xi^{\sigma}_{a_1^\sigma\cdots a_{N_e^\sigma}^\sigma}(\mathbf{r}_1,\ldots,\mathbf{r}_{N_e^\sigma};\mathbf{R}) = \frac{1}{\sqrt{N_e^\sigma!}}\begin{vmatrix} \chi^\sigma_{a_1^\sigma}(\mathbf{r}_1;\mathbf{R}) & \cdots & \chi^\sigma_{a_1^\sigma}(\mathbf{r}_{N_e^\sigma};\mathbf{R}) \\ \vdots & & \vdots \\ \chi^\sigma_{a_{N_e^\sigma}^\sigma}(\mathbf{r}_1;\mathbf{R}) & \cdots & \chi^\sigma_{a_{N_e^\sigma}^\sigma}(\mathbf{r}_{N_e^\sigma};\mathbf{R}) \end{vmatrix}. \quad (38)$$

These adiabatic many-particle states are determined by arbitrary occupied single-particle states.

The set of indices

$$\{a_j^\sigma\} = \{a_1^\sigma\cdots a_{N_e^\sigma}^\sigma\} \quad (39)$$

unambiguously defines these configurations, i.e., the contributing (actually occupied) states $\{\chi^\sigma_{a_j^\sigma}\}$ in (38) belonging to the adiabatic basis $\{\chi_a^\sigma\}$. For the following, it is convenient to introduce the occupation numbers

$$c_a^{j\sigma} = \delta_{a,a_j^\sigma}, \quad (40)$$

which allow us to select from the total set $\{\chi_a^\sigma\}$ the contributing orbitals in (38),

$$\begin{aligned}\chi^\sigma_{a_j^\sigma}(\mathbf{r};\mathbf{R}) &= \sum_a c_a^{j\sigma}\chi_a^\sigma(\mathbf{r};\mathbf{R}) \\ &= \sum_a\sum_\alpha c_a^{j\sigma}U^\sigma_{a\alpha}(\mathbf{R})\phi_\alpha(\mathbf{r}-\mathbf{R}_{A_\alpha}) \\ &\equiv \sum_\alpha c_\alpha^{j\sigma}(\mathbf{R})\phi_\alpha(\mathbf{r}-\mathbf{R}_{A_\alpha}), \end{aligned} \quad (41)$$

with

$$c_\alpha^{j\sigma}(\mathbf{R}) = \sum_a U^\sigma_{a\alpha}(\mathbf{R})c_a^{j\sigma} \quad (42)$$

being their expansion coefficients in local basis-set representation.

With this, the electronic densities $\rho_{\{a_j^\sigma\}} \equiv \rho(\mathbf{r})$ belonging to the many-particle states in (38) read

$$\rho(\mathbf{r}) = \sum_{\sigma=\uparrow\downarrow}\sum_{j=1}^{N_e^\sigma}\sum_{\alpha\beta} c_\alpha^{j\sigma *}(\mathbf{R})c_\beta^{j\sigma}(\mathbf{R})\phi_\alpha^*(\mathbf{r}-\mathbf{R}_{A_\alpha})\phi_\beta(\mathbf{r}-\mathbf{R}_{A_\beta}). \quad (43)$$

They depend implicitly on time via the classical trajectories $\mathbf{R}_{A_\alpha}(t)$. The ground-state density (34) is a special case of (43) with $c_a^{j\sigma} = \delta_{j,a_j^\sigma}$ in (42) and $j = 1,\ldots,N_e^\sigma$ being the lowest adiabatic single-particle levels.

The potential-energy surfaces $E_{\{a_j^\sigma\}}(\mathbf{R}) \equiv E(\mathbf{R})$ belonging to the many-particle states in (38) are given by

$$\begin{aligned} E(\mathbf{R}) = &\sum_{\sigma=\uparrow\downarrow}\sum_{j=1}^{N_e^\sigma}\sum_{\alpha\beta} c_\alpha^{j\sigma *}(\mathbf{R})\Big[T_{\alpha\beta}+V_{\alpha\beta} \\ &+\frac{1}{2}\sum_{\sigma'=\uparrow\downarrow}\sum_{j'=1}^{N_e^{\sigma'}}\sum_{\gamma\delta} Q_{\alpha\beta\gamma\delta}c_\gamma^{j'\sigma' *}(\mathbf{R})c_\delta^{j'\sigma'}(\mathbf{R})\Big]c_\beta^{j\sigma}(\mathbf{R}) \\ &+E_{\rm xc}[\rho](\mathbf{R})+U(\mathbf{R}) \end{aligned} \quad (44)$$

with the matrix elements (27)–(29) and the exchange correlation energy $E_{\rm xc}[\rho](\mathbf{R})$. In (44), $U(\mathbf{R})$ is the field-free classical interaction potential, i.e., the nuclear-nuclear repulsion [Eq. (4) without the laser field].

2. Equations of motion

The electron dynamics is furthermore settled by the time-dependent KS equations of the NA-QMD (30), while the nuclei are moving, still completely independently, on the time-independent potential-energy surfaces $E(\mathbf{R}) = E_{\{a_j^\sigma\}}(\mathbf{R})$, Eq. (44). We thus have

$$\dot a_\alpha^{j\sigma} = -\sum_{\beta\gamma} S^{-1}_{\alpha\beta}\left(iH^\sigma_{\beta\gamma}+B_{\beta\gamma}\right)a_\gamma^{j\sigma}, \quad (45)$$

$$M_A\ddot{\mathbf{R}}_A = -\frac{\partial E(\mathbf{R})}{\partial \mathbf{R}_A}. \quad (46)$$

The electronic EOM (45) are obviously formally the same as in the NA-QMD case (30). Their solution, however, is different from that of (30) because the nuclear trajectories $\mathbf{R}(t)$ are now given by (46) instead of (31).

The physical transparent nuclear EOM (46) are formally different from those given in [21] for the adiabatic QMD case [Eq. (A12) in Ref. [21]], where they are explicitly expressed in local basis-set representation. However, one can easily show that Eq. (46) here and Eq. (A12) in Ref. [21] are identical as long as $E(\mathbf{R})$ belongs to the electronic ground state. In the generalized nuclear EOM (46), however, all electronic adiabatic many-particle states $E(\mathbf{R}) = E_{\{a_j^\sigma\}}(\mathbf{R})$ can occur, whereby the actual surface $E(\mathbf{R})$ is selected randomly during the time evolution by means of Tully's fewest switching algorithm, as described in the next section.

3. Trajectory surface hopping

In order to define the switching probabilities for the hopping algorithm, we expand the time-dependent single-particle Kohn-Sham functions into the adiabatic single-particle states $\chi_a^\sigma(\mathbf{r};\mathbf{R})$ as (see also Fig. 1)

$$\Psi^{j\sigma}(\mathbf{r},t) = \sum_a a_a^{j\sigma}(t)\chi_a^\sigma(\mathbf{r};\mathbf{R}). \quad (47)$$

Analogously, the time-dependent many-particle state for each spin σ,

$$\Psi^\sigma(\mathbf{r}_1,\ldots,\mathbf{r}_{N_e^\sigma},t) = \frac{1}{\sqrt{N_e^\sigma!}}\begin{vmatrix} \Psi^{1\sigma}(\mathbf{r}_1,t) & \cdots & \Psi^{1\sigma}(\mathbf{r}_{N_e^\sigma},t) \\ \vdots & & \vdots \\ \Psi^{N_e^\sigma\sigma}(\mathbf{r}_1,t) & \cdots & \Psi^{N_e^\sigma\sigma}(\mathbf{r}_{N_e^\sigma},t) \end{vmatrix}, \quad (48)$$

is expanded into the adiabatic many-particle states (38), $\Xi^\sigma_{\{a_j^\sigma\}}(\mathbf{r}_1,\ldots,\mathbf{r}_{N_e^\sigma};\mathbf{R})$, as

$$\Psi^\sigma(\mathbf{r}_1,\ldots,\mathbf{r}_{N_e^\sigma},t) = \sum_{a_1^\sigma<\cdots<a_{N_e^\sigma}^\sigma} C^\sigma_{\{a_j^\sigma\}}(t) \times \Xi^\sigma_{\{a_j^\sigma\}}(\mathbf{r}_1,\ldots,\mathbf{r}_{N_e^\sigma};\mathbf{R}). \quad (49)$$

The time-dependent many-particle expansion coefficients $C^\sigma_{\{a_j^\sigma\}}(t)$ are determinants of the time-dependent expansion coefficients $a_a^{j\sigma}(t)$ in (47) with the lower index $a \equiv a_k^\sigma$ and the upper index j running from $k = 1$ and $j = 1$ up to $k = N_e^\sigma$

and $j = N_e^\sigma$ for the actual configuration $\{a_j^\sigma\}$,

$$C^\sigma_{\{a_j^\sigma\}}(t) = \begin{vmatrix} a^{1\sigma}_{a_1^\sigma}(t) & \cdots & a^{N_e^\sigma\sigma}_{a_1^\sigma}(t) \\ \vdots & & \vdots \\ a^{1\sigma}_{a_{N_e^\sigma}^\sigma}(t) & \cdots & a^{N_e^\sigma\sigma}_{a_{N_e^\sigma}^\sigma}(t) \end{vmatrix}. \tag{50}$$

The time-dependent coefficients $a_a^{j\sigma}(t)$ in (50) are obtained from the time-dependent single-particle coefficients of the atomic basis $a_\alpha^{j\sigma}(t)$, resulting from the EOM (45), via the transformation (see also Fig. 1)

$$a_a^{j\sigma}(t) = \sum_{\alpha\beta} U^{\sigma+}_{\alpha a}(\mathbf{R}) S_{\alpha\beta} a_\beta^{j\sigma}(t). \tag{51}$$

In order to tag quantities which depend on two configurations, $\{a_j^\sigma\}$ and $\{b_j^\sigma\}$, we introduce the abbreviation in the indices,

$$\left\{a_j^\sigma, b_j^\sigma\right\} = a_1^\sigma \cdots a_{N_e^\sigma}^\sigma, b_1^\sigma \cdots b_{N_e^\sigma}^\sigma. \tag{52}$$

Now, according to Tully's hopping procedure [40], the transition probabilities $g^\sigma_{\{a_j^\sigma, b_j^\sigma\}}$ from a given state $\Xi^\sigma_{\{a_j^\sigma\}}$, i.e., the actual surface $E(\mathbf{R}) = E_{\{a_j^\sigma\}}(\mathbf{R})$ in the nuclear EOM (46) at time t, to an arbitrary state $\Xi^\sigma_{\{b_j^\sigma\}}$ at time $t + \Delta t$ [with Δt being the numerical time step of solving (46)] is given by

$$g^\sigma_{\{a_j^\sigma, b_j^\sigma\}} = \frac{B^\sigma_{\{b_j^\sigma, a_j^\sigma\}}}{A^\sigma_{\{a_j^\sigma, a_j^\sigma\}}} \Delta t, \tag{53}$$

with

$$A^\sigma_{\{a_j^\sigma, b_j^\sigma\}} = C^{\sigma *}_{\{a_j^\sigma\}} C^\sigma_{\{b_j^\sigma\}} \tag{54}$$

and

$$\begin{aligned} B^\sigma_{\{a_j^\sigma, b_j^\sigma\}} = &-2\mathrm{Re}\left(A^\sigma_{\{a_j^\sigma, b_j^\sigma\}} D^\sigma_{\{a_j^\sigma, b_j^\sigma\}}\right) \\ &- 2\mathrm{Im}\left(A^\sigma_{\{a_j^\sigma, b_j^\sigma\}} L^\sigma_{\{a_j^\sigma, b_j^\sigma\}}\right). \end{aligned} \tag{55}$$

In (55), the many-electron nonadiabatic coupling $D^\sigma_{\{a_j^\sigma, b_j^\sigma\}}$ and laser-induced diabatic coupling $L^\sigma_{\{a_j^\sigma, b_j^\sigma\}}$ given by

$$D^\sigma_{\{a_j^\sigma, b_j^\sigma\}} = \left\langle \Xi^\sigma_{\{a_j^\sigma\}} \middle| \frac{d}{dt} \Xi^\sigma_{\{b_j^\sigma\}} \right\rangle = \dot{\mathbf{R}} \left\langle \Xi^\sigma_{\{a_j^\sigma\}} \middle| \frac{\partial}{\partial \mathbf{R}} \Xi^\sigma_{\{b_j^\sigma\}} \right\rangle, \tag{56}$$

$$L^\sigma_{\{a_j^\sigma, b_j^\sigma\}} = \left\langle \Xi^\sigma_{\{a_j^\sigma\}} \middle| \mathbf{r} \cdot \mathbf{E}(t) \middle| \Xi^\sigma_{\{b_j^\sigma\}} \right\rangle = \mathbf{E}(t) \cdot \left\langle \Xi^\sigma_{\{a_j^\sigma\}} \middle| \mathbf{r} \middle| \Xi^\sigma_{\{b_j^\sigma\}} \right\rangle, \tag{57}$$

respectively, are nonzero only in the case of a one-particle transition, i.e., when the states $\Xi^\sigma_{\{a_j^\sigma\}}$ and $\Xi^\sigma_{\{b_j^\sigma\}}$ differ in exactly one orbital. The hopping criterion is then formulated as a comparison with a uniform random number ζ ($0 \leqslant \zeta \leqslant 1$): A hop for spin σ from state $\Xi^\sigma_{\{a_j^\sigma\}}$ to state $\Xi^\sigma_{\{b_j^\sigma\}}$ occurs if

$$\sum_{b_1'^\sigma < \cdots < b'^\sigma_{N_e^\sigma}}{}' g^\sigma_{\{a_j^\sigma, b_j'^\sigma\}} < \zeta < \sum_{b_1'^\sigma < \cdots < b'^\sigma_{N_e^\sigma}} g^\sigma_{\{a_j^\sigma, b_j'^\sigma\}}, \tag{58}$$

where the primed sum denotes summation over all energy levels below (excluding) the total adiabatic many-particle energy $E_{\{b_j^\sigma\}}$ and the full sum denotes summation over all energy levels up to (including) the total adiabatic many-particle energy $E_{\{b_j^\sigma\}}$ accessible via one-particle excitations from the initial state $E_{\{a_j^\sigma\}}$. As a consequence, many-particle transitions are realized as successive one-particle transitions (for an illustration see Fig. 2).

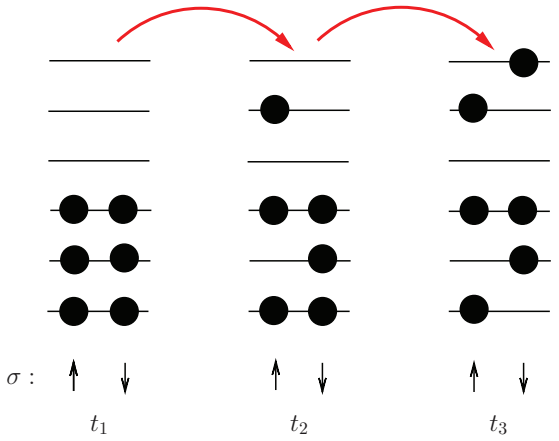

FIG. 2. (Color online) Schematic representation of the surface-hopping procedure in the adiabatic many-electron picture. Initially, at time t_1, the system is in its ground state. At some later time t_2, a hop occurs, leading to a singly excited state, and even later, another hop occurs, and the system ends up in a doubly excited state. In this way, many-particle transitions are realized as successive one-particle transitions. Defining the single-particle occupation configuration for each spin as $p_a^\sigma = \sum_{j=1}^{N_e} c_a^{j\sigma}$ [see (40)], we get a simple representation of the adiabatic many-electron states: $\{p^\uparrow\} = (111000)$ and $\{p^\downarrow\} = (111000)$ at t_1, $\{p^\uparrow\} = (101010)$ and $\{p^\downarrow\} = (111000)$ at t_2, $\{p^\uparrow\} = (101010)$ and $\{p^\downarrow\} = (011001)$ at t_3, etc.

When a hop for spin σ occurs, the kinetic energy has to be adapted in order to guarantee total energy conservation. In the simplest way, this can be done by rescaling all classical velocity components by a common factor connected to the ratio of the kinetic energy after and before the hop. A more refined, but computationally much more demanding, way is to rescale the classical velocity components along the nonadiabatic coupling vector in (56):

$$\mathbf{D}^\sigma_{\{a_j^\sigma, b_j^\sigma\}} = \left\langle \Xi^\sigma_{\{a_j^\sigma\}} \middle| \frac{\partial}{\partial \mathbf{R}} \Xi^\sigma_{\{b_j^\sigma\}} \right\rangle. \tag{59}$$

If the classical kinetic energy is not sufficient to perform a transition, then the hop is just rejected. In the presence of the laser field the kinetic energy adaption is not applied because the energy is not conserved.

With the electronic EOM (45), the nuclear EOM (46), the hopping probabilities (58), and the chosen velocity rescaling method the essentials of the NA-QMD-H approach are formulated. The method represents a *trajectory-surface-hopping* approach for atomic many-body systems. The nuclear dynamics do not proceed purely classically due to the nonclassical, probabilistic transitions between potential-energy surfaces.

4. Remarks and comparison to other approaches

In this section a critical discussion of the approximations, assumptions, advantages, and restrictions of the presented method is given, along with a comparison to existing *ab initio* MD procedures based on TD-DFT combined with Tully hopping [36–38].

All three approaches [36–38] differ considerably from each other (see discussion below). Common, however, to all of them is the use of the plane-wave basis expansion for the KS orbitals. This considerably restricts the range of applications and prevents one from describing, for example, atomic collisions and the following fragmentation processes. In contrast, the heart of our method is based on a local atomic basis expansion, allowing us to handle such situations (see paper II of this series). In addition, as an extension to [36–38], it allows us to take into account explicitly a laser field (see paper III of this series). Finally, the present NA-QMD-H approach can be extended to describe and include even ionization (see item (v) below).

The following details are critically discussed and compared.

(i) The electronic excitation energies (44) and thus the forces on the nuclei (46) are based on bare KS excitations, as used in [37]. These excitation energies have been shown to be well-defined approximations [67] to the more accurate excitation energies, calculated, e.g., within linear response TD-DFT [38]. A detailed discussion of this point has also been given in [68].

In addition, the KS excitations allow the inclusion of, in principle, an unlimited number of excited states, overcoming the limitations of restricted open-shell KS excitations [36], which are capable of treating only the lowest-lying states. As another advantage, multiply excited states, which are important in the photoisomerization of ethylene [33,49], can be treated by KS excitations, whereas linear response TD-DFT only allows one to treat one-particle excitations.

From the numerical point of view, the calculation of the nonadiabatic couplings (56) and diabatic couplings (57) is very efficient with KS excitations, as those between adiabatic Slater determinants are nonzero only in the case of one-particle transitions. Thus, the NA-QMD-H method should allow us to treat rather large systems at *relatively* moderate computational cost.

We also note that it is crucial to keep track of the adiabatic states between successive time steps. This will be done using a sign consistency procedure based on the maximal delayed overlap of the adiabatic states, in analogy to [69].

(ii) As in all approaches in [36–38], we take the electronic ground state of the system as a reference for the adiabatic states (38) and the Tully hopping procedure (58), which minimizes the number of hops for a single trajectory (fewest switches algorithm [40]). However, this choice will limit the application of the theory to short laser pulses, which indeed may induce electronic excitations via (57) but, on the other hand, must be short enough that they do not affect the nuclear motion considerably. For longer pulses, the explicit inclusion of the laser field requires an improved treatment, e.g., the use of time-dependent Floquet states [70] instead of the adiabatic surfaces, which are also used in [71]. This, however, clearly goes beyond the scope of the present work.

(iii) As a peculiarity of our hopping method, we treat both spins separately, as usually done in conventional HF or LSDA calculations. Nevertheless, the separate hopping procedure for both spins represents an approximation, as the action (6) is not separable with respect to the spin contributions. Note, however, that both spin systems are still coupled via the total many-particle energies (44), which depend on both spins and build the foundation for the hopping criterion (58). Needless to say, an explicit treatment of a possible time-dependent magnetic field requires a coupled treatment of both spin contributions in the hopping algorithm.

(iv) Instead of a classical path approximation [37], we treat electronic and nuclear dynamics as being self-consistently coupled. This will allow us to study in the future, in addition to electronic relaxation processes and/or isomerization mechanisms, a large variety of other nonadiabatic phenomena on this level of approximations, e.g., large-amplitude vibrational motion [30], scattering between complex particles [28,29], fragmentation in laser fields [51,54], etc.

(v) In principle, the present NA-QMD-H formalism can be extended to include also ionization processes by including ionized surfaces in the hopping procedure, i.e., ionized Born-Oppenheimer surfaces in the case of collisions and ionized Floquet surfaces in the case of laser interaction. In clear contrast to the (mean-field) NA-QMD formalism including ionization [41], such a theory would offer the possibility to decide explicitly between single-, double-, and higher-ionization channels. Its development represents a great challenge for the future.

The validity and accuracy of all assumptions and approximations will depend on the system under study. Despite that, however, the NA-QMD-H method offers a simple and straightforward extension of the NA-QMD approach, which, in principle, makes it possible to take into account quantum effects in the nuclear motion for systems with a large number of atoms and electrons.

C. Adiabatic quantum molecular dynamics and hierarchy of *ab initio* MD methods

In summary, we have discussed three types of *ab initio* MD methods:

(i) By definition, adiabatic QMD describes *classical nuclear motion* on the Born-Oppenheimer ground-state surface calculated by any *ab initio*, *quantum electronic* structure method, i.e., time-independent DFT or HF in our case [43,58].

(ii) The NA-QMD method includes electronic excitations but still treats the nuclei classically moving on an effective, explicitly time-dependent potential (Ehrenfest dynamics) [22,41–43].

(iii) The present NA-QMD-H approach, in addition, accounts approximately for quantum effects in the nuclear dynamics by using Tully's surface-hopping procedure.

Thus, all three MD methods represent a kind of hierarchy of *ab initio* MD approaches with increasing complexity and generality (see Fig. 3).

On the other hand, both nonadiabatic approaches should automatically contain the adiabatic QMD limit if electronic transitions are unlikely or unimportant. In [21] we have explicitly shown that the EOM of the QMD can be derived from those of the NA-QMD method (31) if the time scales of electronic and nuclear dynamics are very different (right arrow in Fig. 3). Evidently, the NA-QMD-H formalism (45), (46), and (58) reduces to the QMD limit if all hopping probabilities (53) vanish (left arrow in Fig. 3).

The circumstances in which this is the case can be entirely recognized by considering the quantities entering the nonadiabatic and diabatic matrix elements (56) and (57),

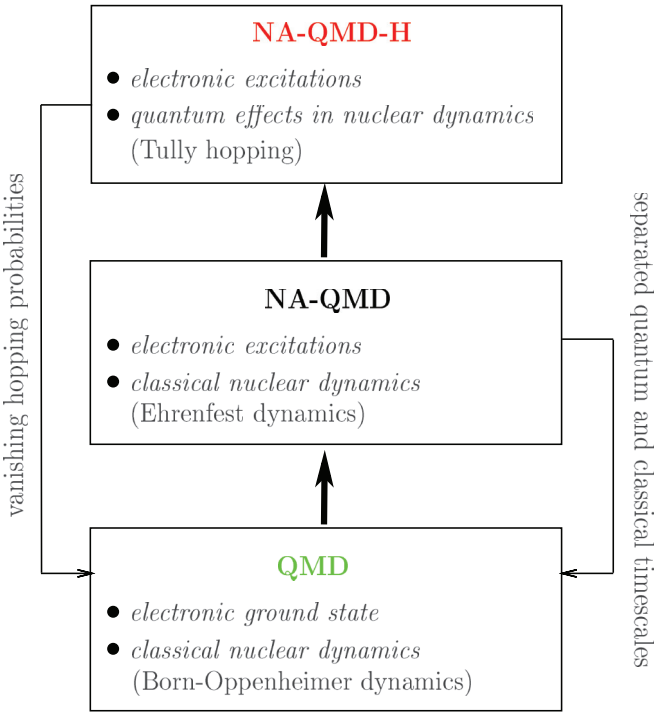

FIG. 3. (Color online) Hierarchy of *ab initio* MD methods: QMD, NA-QMD, and NA-QMD-H. The left and right linkages indicate that both nonadiabatic approaches naturally merge into the adiabatic QMD limit under certain conditions (see text).

which determine the hopping probabilities (53). This concerns the nuclear velocities $\dot{\mathbf{R}}$ in (56) and the electric field $\mathbf{E}$ in (57) (as external dynamical parameters for the electrons) as well as the nonadiabatic coupling vector in (56) and the dipole transition matrix element in (57) (as inherent electronic structure properties). Thus, electronic transitions can be suppressed for four reasons:

(i) If the nuclear velocities $\dot{\mathbf{R}}$ in (56) and thus the kinetic energy of the nuclei are too small, electronic excitations are forbidden by energy conservation as an inherent part of the hopping procedure.

(ii) Energetically allowed hops are strongly suppressed if the nonadiabatic coupling matrix elements (56) vanish; that is, avoided crossings or conical intersections in the adiabatic potential-energy surfaces (44) are lacking.

(iii) A laser field induces transitions only if the field strength $\mathbf{E}$ (or intensity) is large enough to create finite hopping probabilities (53) via (57) because the field is described classically in the formalism.

(iv) Even the strongest field strength $\mathbf{E}$ is not enough to create transitions as long as the dipole matrix elements in (57) vanish owing to symmetry reasons.

Thus, the NA-QMD-H formalism also provides a physical transparent picture of the complex nonadiabatic mechanisms.

III. CASE STUDY: MODEL SYSTEM OF $H^+ + H$ COLLISIONS

In order to obtain insight into the mechanism and consequences of the electron-nuclear correlations in nonadiabatic dynamics, we consider here the simplest case: an idealized two-state model of $H^+ + H$ collisions, which is described in detail below. The fundamental one-electron system, $H^+ + H$, or $H_2{}^+$, already served as a case study in our previous work on collisions [21] and laser-molecule interaction [22]. Although this model has little to do with reality, it is particularly well suited to deliver a transparent and pedagogically useful insight into the complex nonadiabatic mechanisms.

Here, we will focus in particular on the basic differences of and the general similarities between the NA-QMD and NA-QMD-H formalisms to reveal some principal effects of electron-nuclear correlations in atomic collisions. In addition, we will compare the predictions of both methods with those of exact quantum-mechanical calculations.

A. Collision model

In order to make the approach as transparent as possible we set up the simplest atomic collision model for the $H_2{}^+$ system (see also [21]): Only central collisions are considered, and a minimal atomic and molecular basis set is used that allows for nonadiabatic transitions.

The electronic Hamiltonian (13) reads

$$H(\mathbf{r};R) = -\frac{\nabla_{\mathbf{r}}^2}{2} - \frac{1}{\left|\mathbf{r}+\frac{R}{2}\mathbf{e}_z\right|} - \frac{1}{\left|\mathbf{r}-\frac{R}{2}\mathbf{e}_z\right|}, \tag{60}$$

and the classical interaction potential (4) is simply given by the Coulomb repulsion

$$U(R) = \frac{1}{R}, \tag{61}$$

with the internuclear distance between the two protons $R = |\mathbf{R}_1 - \mathbf{R}_2|$ and the collision axis $\mathbf{e}_z$.

In this case, the classical EOM of the NA-QMD (31) and NA-QMD-H (46) reduce to a one-dimensional problem for the internuclear distance R. The corresponding time-dependent KS equations (30) and (45) reduce to the time-dependent Schrödinger equation for the expansion coefficients of the one-particle wave function $\Psi^{j\sigma}(\mathbf{r},t) \equiv \Phi(\mathbf{r},t)$ in the atomic basis expansion (15). However, here, we use an adiabatic molecular basis expansion [Eq. (47)] for the representation of $\Phi(\mathbf{r},t)$. This allows us to perform exact quantum–mechanical, NA-QMD and NA-QMD-H calculations on equal footing.

The *adiabatic* molecular states $\chi_a^\sigma(\mathbf{r};R) \equiv \Phi_n(\mathbf{r};R)$ and the corresponding energy levels $\epsilon_a^\sigma(R) \equiv E_n(R)$ in (32) are obtained from the solution of (37) by intentionally using the smallest possible set of atomic hydrogen orbitals ϕ_α in (36) that may lead to excitations, i.e., the $1s$ and $2s$ functions centered on both nuclei, generating the four molecular states $1s\sigma_u$ ($n=1$), $2s\sigma_u$ ($n=2$), $1s\sigma_g$, and $2s\sigma_g$. Both σ_g states are then excluded in our model for two reasons: First, the σ_g states are essentially decoupled from the σ_u states and exhibit only a small nonadiabatic coupling; second, in doing so, we end up at the minimal collision model of $H^+ + H$ exhibiting only two molecular states. The primary nonadiabatic mechanism remains unaffected by this choice, while the model is kept as simple as possible. The energy levels $E_n(R)$ are shown in Fig. 4(a) (solid black curves). These states exhibit only one avoided crossing at $R \approx 0.8$ a.u., which is connected with a

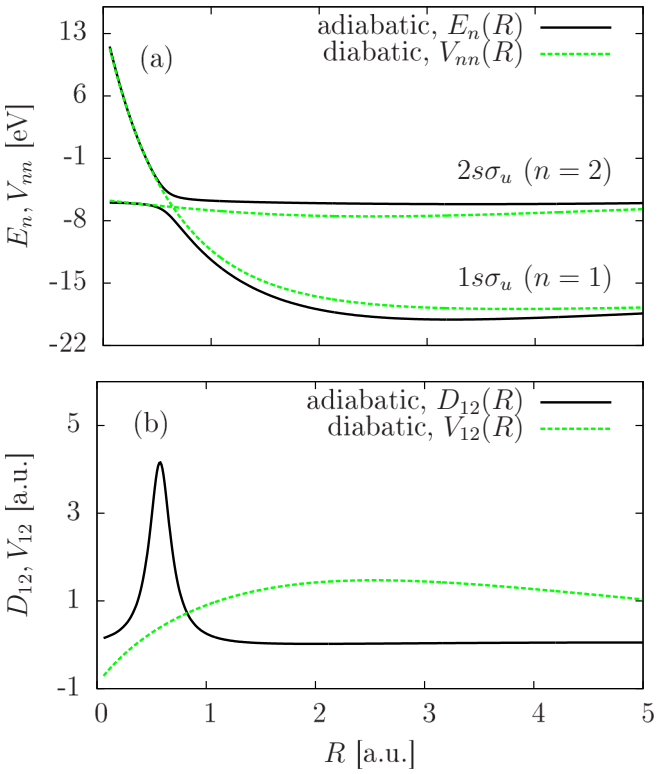

FIG. 4. (Color online) (a) Energy levels of H_2^+ in the adiabatic and diabatic representation as well as (b) the respective couplings as a function of the internuclear distance R. They are obtained from QMD ground-state calculations using the Gaussian basis set d-aug-cc-pV6Z (see [55–57]) for numerical construction of the $1s$ and $2s$ atomic orbitals of hydrogen. Only the $1s\sigma_u$ and $2s\sigma_u$ states are considered, as discussed in the text.

large nonadiabatic coupling

$$D_{12}(R) = \langle \Phi_1(\mathbf{r};R)|\frac{\partial}{\partial R}|\Phi_2(\mathbf{r};R)\rangle, \tag{62}$$

as shown by the solid black curve in Fig. 4(b). This gives rise to the following nonadiabatic mechanism: starting initially on the lower potential-energy surface ($1s\sigma_u$ state) at large R, the system crosses the nonadiabatic transition region twice in the course of the collision dynamics, where the avoided crossing may give rise to nonadiabatic transitions between both surfaces.

The corresponding *diabatic* molecular basis set $\{\tilde{\Phi}_n(\mathbf{r};R)\}$ provides a convenient framework for exact quantum-mechanical calculations and is derived from the adiabatic basis set $\{\Phi_n(\mathbf{r};R)\}$ by the so-called Smith rotation [72]

$$\begin{pmatrix}\tilde{\Phi}_1(\mathbf{r};R)\\ \tilde{\Phi}_2(\mathbf{r};R)\end{pmatrix} = \begin{pmatrix}\cos\theta(R) & \sin\theta(R)\\ -\sin\theta(R) & \cos\theta(R)\end{pmatrix}\begin{pmatrix}\Phi_1(\mathbf{r};R)\\ \Phi_2(\mathbf{r};R)\end{pmatrix} \tag{63}$$

under the condition of vanishing derivative couplings

$$\langle\tilde{\Phi}_1(\mathbf{r};R)|\frac{\partial}{\partial R}|\tilde{\Phi}_2(\mathbf{r};R)\rangle = 0. \tag{64}$$

Correspondingly, the Smith rotation $\theta(R)$ angle is given by

$$\theta(R) = \int_R^\infty dR' D_{12}(R'). \tag{65}$$

According to the orthogonal transformation (63), the corresponding diabatic energy levels $V_{nn}(R)$ and their respective coupling $V_{12}(R)$ are connected with the respective adiabatic quantities by

$$V_{11}(R) = \cos^2\theta(R)E_1(R) + \sin^2\theta(R)E_2(R), \tag{66}$$

$$V_{22}(R) = \sin^2\theta(R)E_1(R) + \cos^2\theta(R)E_2(R), \tag{67}$$

$$V_{12}(R) = V_{21}(R) = [E_1(R) - E_2(R)]\cos\theta(R)\sin\theta(R). \tag{68}$$

The diabatic energy levels $V_{nn}(R)$ and their coupling $V_{12}(R)$ are also shown in Fig. 4 (green dashed curves). In contrast to the adiabatic energy levels $E_n(R)$, the diabatic energy levels cross in the nonadiabatic transition region [Fig. 4(a)], whereas their coupling spreads over a large R region compared to the strongly localized coupling $D_{12}(R)$ in the adiabatic framework [Fig. 4(b)].

We will consider two quantities (observables): first, the mean total kinetic-energy loss ΔE of the colliding system as a function of the center-of-mass impact energy $E_{\rm cm}$, which in this case is equal to the mean transferred electronic excitation energy at a given $E_{\rm cm}$ due to the lack of internal vibrational DOF, and, second, the differential kinetic-energy spectra of both nuclei $P(E)$, i.e., the probability of measuring the relative kinetic energy E between the nuclei in the exit channel.

B. Exact quantum-mechanical calculations

The one-electron nature of the collision model allows us to perform relatively easy exact quantum-mechanical calculations for the whole collision system. For this purpose, the diabatic representation is the convenient and practical framework (see above). Therefore, we expand the total wave function into the diabatic basis,

$$\Psi(\mathbf{r},R,t) = \sum_{n=1}^{2}\Omega_n(R,t)\tilde{\Phi}_n(\mathbf{r};R). \tag{69}$$

Using this, we derive the coupled time-dependent Schrödinger equations for the nuclear wave function $\Omega_n(R,t)$,

$$i\frac{\partial}{\partial t}\Omega_n(R,t) = \left[-\frac{1}{2\mu}\frac{\partial^2}{\partial R^2} + \frac{1}{R}\right]\Omega_n(R,t) + \sum_{m=1}^{2}V_{nm}(R)\Omega_m(R,t), \tag{70}$$

with the reduced mass $\mu = 918.0$ a.u.

The initial state is chosen as a traveling Gaussian starting from the $1s\sigma_u$ surface,

$$\Omega_1(R,t=0) = \left(\frac{\pi\sigma^2}{2}\right)^{\frac{1}{4}} e^{i(R-R_0)P_{R_0} - \frac{(R-R_0)^2}{4\sigma^2}}, \tag{71}$$

with width $\sigma = 0.7$ a.u., $R_0 = 20.0$ a.u., and an initial momentum $P_{R_0} = -\sqrt{2\mu E_{\rm cm}}$ corresponding to the mean impact energy $E_{\rm cm}$ of the wave packet.

Equation (70) is then solved numerically using the code WAVEPACKET [73] by expanding the nuclear wave function in a basis of plane waves and applying the split-operator scheme [74]. We use an equally spaced radial grid with 2000 grid points ranging from 0.06 to 32.0 a.u. The time step is $\Delta t = 0.1$ a.u. The final time is set to $t_{\rm f} \approx \frac{\mu}{|P_{R_0}|} \times 40.0$ a.u., which represents an estimate of the return of the wave packet to its initial center.

The mean kinetic-energy loss

$$\Delta E = \bar{E}_{\rm kin}(t=0) - \bar{E}_{\rm kin}(t_{\rm f}) \tag{72}$$

is calculated from the expectation values of the kinetic energy

$$\bar{E}_{\rm kin}(t) = \sum_n \int_{R=0}^{\infty} dR\, \Omega_n^*(R,t) \left[-\frac{1}{2\mu} \frac{\partial^2}{\partial R^2} \right] \Omega_n(R,t), \tag{73}$$

with $\bar{E}_{\rm kin}(t=0) \equiv E_{\rm cm}$. The differential kinetic-energy spectrum $P(E)$ of the nuclei is obtained from the momentum representation of the nuclear wave function at $t = t_{\rm f}$ as

$$P(E) = \frac{1}{2\pi} \sum_n \left| \int_{R=0}^{\infty} dR e^{i\sqrt{2\mu E}R} \Omega_n(R,t_{\rm f}) \right|^2. \tag{74}$$

C. NA-QMD calculations

In contrast to the exact quantum-mechanical approach (see above), the nuclear degrees of freedom are treated classically in NA-QMD and NA-QMD-H. In these methods, the adiabatic basis expansion (47) of the electronic wave function reads

$$\Phi(\mathbf{r},t) = \sum_{n=1}^{2} a_n(t) \Phi_n(\mathbf{r};R), \tag{75}$$

with the adiabatic expansion coefficients $a_a^{j\sigma}(t) \equiv a_n(t)$. In the case of the NA-QMD approach, this leads to the mixed quantum-classical equations of motion,

$$\dot{a}_n(t) = -i E_n(R) a_n(t) - \sum_{m=1}^{2} \dot{R} D_{nm}(R) a_m(t), \tag{76}$$

$$\dot{P}_R = -\frac{\partial E^{\rm surf}(t)}{\partial R} - \sum_{n,m=1}^{2} a_n^*(t) a_m(t) [E_n(R) - E_m(R)] D_{nm}(R), \tag{77}$$

$$\dot{R} = \frac{P_R}{\mu}, \tag{78}$$

with the *effective time-dependent* potential-energy surface [see (26)], except now in the adiabatic representation,

$$E(t) \equiv E^{\rm surf}(t) = \sum_{n=1}^{2} |a_n(t)|^2 E_n(R) + \frac{1}{R}. \tag{79}$$

The initial state is an ensemble of classical trajectories starting from the $1s\sigma_{\rm u}$ surface, i.e., $a_1(t=0) = 1$. The initial internuclear distances R and momenta P_R are chosen randomly according to the Wigner distribution $W(R,P_R)$ of the quantum-mechanical initial state (71),

$$W(R,P_R) = \frac{1}{2\pi} e^{-\frac{(R-R_0)^2}{2\sigma^2}} e^{-2\sigma^2 (P_R - P_{R_0})^2}, \tag{80}$$

corresponding to the central impact energy $E_{\rm cm} = \frac{P_{R_0}^2}{2\mu}$, the mean initial distance $R_0 = 19.0$ a.u., and $\sigma = 0.7$ a.u., as in (71). This allows a meaningful comparison of the differential kinetic-energy spectra $P(E)$ with the quantum-mechanical spectra (74).

Equations (76)–(78) are integrated using a fourth-order Runge-Kutta scheme with a time step $\Delta t = 0.01$ a.u. The final time $t_{\rm f}$ is defined by $R(t_{\rm f}) = R_0$, i.e., the return of the trajectory to its starting point after scattering. For convergence, a total of $N_{\rm traj} = 1000$ trajectories with different initial conditions R and P_R for each impact energy $E_{\rm cm}$ is sufficient.

The kinetic-energy loss is given by

$$\Delta E = E_{\rm cm} - \bar{E}_{\rm kin}(t_{\rm f}), \tag{81}$$

where $\bar{E}_{\rm kin}(t_{\rm f}) = \frac{1}{N_{\rm traj}} \sum_{\rm trajectories} \frac{P_R(t_{\rm f})^2}{2\mu}$ is the mean kinetic energy in the exit channel. The kinetic-energy spectrum $P(E)$ is obtained from a smoothed histogram of the final kinetic energies $E = \frac{P_R(t_{\rm f})^2}{2\mu}$ corresponding to different initial conditions.

D. NA-QMD-H calculations

Analogously, starting from the basis expansion (75), the equations of motion for the NA-QMD-H method are given by

$$\dot{a}_n(t) = -i E_n(R) a_n(t) - \sum_{m=1}^{2} \dot{R} D_{nm}(R) a_m(t), \tag{82}$$

$$\dot{P}_R = -\frac{\partial E_n^{\rm surf}(R)}{\partial R}, \quad n = 1 \text{ or } 2, \tag{83}$$

$$\dot{R} = \frac{P_R}{\mu}, \tag{84}$$

with the *actual time-independent* potential-energy surface [see (44)]

$$E_{a_1 \cdots a_{N_e}} \equiv E_n^{\rm surf}(R) = E_n(R) + \frac{1}{R}. \tag{85}$$

The change of the surface is enabled via Tully hopping, and the general quantities (53), (54), and (55), as defined in Sec. II B, reduce to

$$g_{nm} = \frac{B_{mn}}{A_{nn}} \Delta t, \tag{86}$$

$$A_{mn} = a_m^* a_n, \tag{87}$$

$$B_{mn} = -2{\rm Re}(A_{mn} D_{mn} \cdot \dot{R}). \tag{88}$$

The system switches from $E_n^{\rm surf}(R)$ to $E_m^{\rm surf}(R)$ if two conditions are fulfilled [see (58)]:

(i) $\zeta < g_{nm}$, where ζ is a uniform random number ($0 \leqslant \zeta \leqslant 1$), and

(ii) there is a sufficient amount of kinetic energy, i.e., $\frac{P_R(t)^2}{2\mu} > E_m^{\rm surf}(R) - E_n^{\rm surf}(R)$.
In the case of a switch, the kinetic energy is adapted by momentum rescaling.

The initial conditions, numerical parameters for solving Eqs. (82)–(84), and the definition of the kinetic-energy loss ΔE and kinetic-energy spectra $P(E)$ are the same as in the NA-QMD calculations (see above). For convergence, however, a total of $N_{\rm traj} = 10\,000$ trajectories for each impact energy $E_{\rm cm}$ is necessary because for each initial condition R and P_R an ensemble of trajectories also has to be considered.

E. Results and discussion

Due to the simplicity of the model (two states with the lower state being the initial one, one avoided crossing passed twice, no internal vibrational DOF), the results, shown in Fig. 5, can be interpreted and understood in detail.

In Fig. 5(a), the mean kinetic-energy loss ΔE as a function of the impact energy $E_{\rm cm}$ is presented. Evidently, the results obtained in all three methods are qualitatively and quantitatively the same. At low impact energy $E_{\rm cm} \lesssim 35$ eV, the collision proceeds elastically with zero energy loss and thus no electronic excitation. With increasing $E_{\rm cm}$, nonadiabatic transitions to the higher potential-energy surface $E_2(R)$ become important, and the energy loss reaches a maximum at $E_{\rm cm} \approx 74$ eV, with $\Delta E \approx 9$ eV almost corresponding to the asymptotic difference in the potential-energy surfaces $E_2(\infty) - E_1(\infty) \approx 10$ eV [see Fig. 4(a)] and thus to the maximal possible energy loss. Hence, this maximum appears due to a constructive interference of electronic transitions of the first and second passings of the nonadiabatic coupling region [with final-state populations $|a_2(t_{\rm f})|^2 \approx 1$ and $|a_1(t_{\rm f})|^2 \approx 0$] and can be qualitatively understood already within Landau-Zener-Stückelberg theory [21,75]. At larger impact energies $E_{\rm cm} \gtrsim 74$ eV, the optimal conditions for this constructive interference disappear, leading to a natural decrease of ΔE with increasing $E_{\rm cm}$ [75]. Summarizing this part, from the present analysis one can conclude that electron-nuclear correlations do not show up as long as integral quantities (like ΔE) are considered.

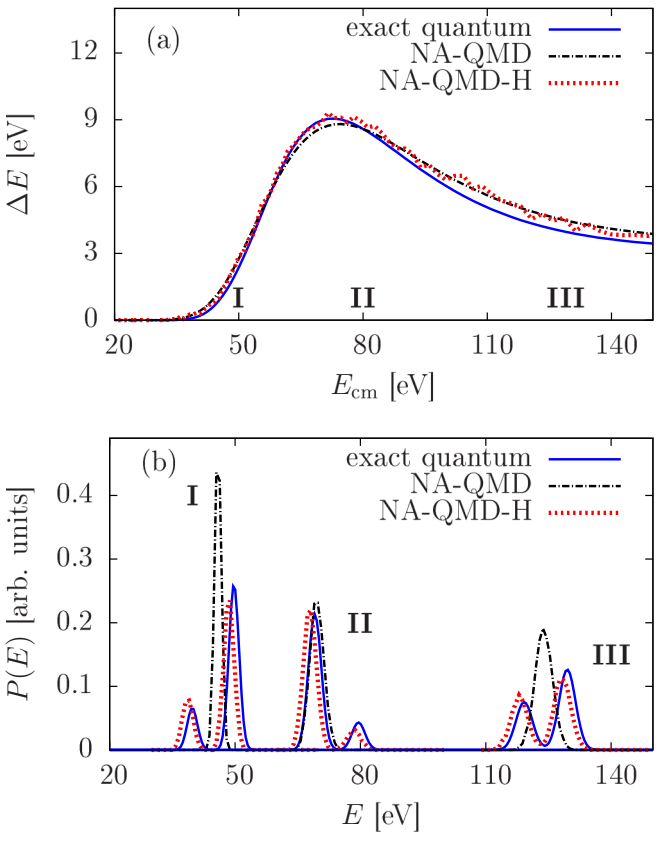

FIG. 5. (Color online) (a) Kinetic-energy loss ΔE as a function of the impact energy $E_{\rm cm}$ and (b) kinetic-energy spectra $P(E)$ taken at the three impact energies indicated in (a): 50 eV (I), 80 eV (II), and 129 eV (III).

The situation changes drastically when more differential quantities, like the kinetic-energy spectra of the nuclei $P(E)$, are considered. In Fig. 5(b), these spectra are shown for three impact energies ($E_{\rm cm} = 50, 80,$ and 129 eV). The (correct) quantum-mechanical results generally exhibit a double-peak structure (corresponding to the two possible reaction channels within the model), with one peak centered at $E_{\rm cm}$ (elastic scattering) and the second one at $E_{\rm cm} - [E_2(\infty) - E_1(\infty)] \approx E_{\rm cm} - 10$ eV (inelastic scattering). Thereby, the relative peak heights measure the degree of inelasticity: In the weakly nonadiabatic region I (with $E_{\rm cm} = 50$ eV and $\Delta E \approx 2.8$ eV), the elastic peak dominates over the inelastic one, whereas the opposite is the case in the optimal transfer region II (with $E_{\rm cm} = 80$ eV and $\Delta E \approx 8.6$ eV). In the high-energy region III (with $E_{\rm cm} = 129$ eV and $\Delta E \approx 4.5$ eV), again, the elastic peak height exceeds the inelastic one.

In contrast (and as expected), the NA-QMD results generally exhibit only one (average) peak, with peak positions, however, corresponding to the mean values of the double-humped quantum-mechanical distributions. The spectra obtained within the NA-QMD-H approach reproduce (somewhat surprisingly) *quantitatively* the exact quantum-mechanical results, demonstrating that for this toy model the surface-hopping mechanism accounts completely for the quantum nature of the nuclear motion.

IV. SUMMARY AND OUTLOOK

In summary, we presented an extension of the NA-QMD method [21,22,41,42] to account for electron-nuclear correlations in the dynamics of finite atomic many-body systems. This scheme, which we term NA-QMD-H, self-consistently couples quantum dynamics for the electrons within TD-DFT (or TD-HF) with trajectory-surface-hopping dynamics for the nuclei and thus approximately accounts for quantum effects in the nuclear dynamics.

We added a detailed and critical discussion of the basic assumptions and possible improvements or extensions of the method. Differences and similarities of the approach compared to other state-of-the-art MD approaches were outlined as well.

We presented a systematic hierarchy of *ab initio* MD approaches with increasing complexity and generality and discussed under which circumstances any nonadiabatic MD merges into the adiabatic QMD limit. Going from bottom to the top in Fig. 3, this hierarchy also suggests that the present formalism of the NA-QMD-H method is the result of a

continuous and systematic extension and generalization of the basic QMD. The ultimate goal in this ongoing development must be to include also quantum coherence effects in the nuclear dynamics.

Finally, intentionally using the simplest possible two-state collision model of $H^+ + H$, we demonstrated exemplarily the relevance of electron-nuclear correlations in atomic collisions by comparing the results of the mean-field NA-QMD and the correlated NA-QMD-H with exact quantum calculations. While both approaches describe mean observables very well (total kinetic-energy loss ΔE as a function of the impact energy E_{cm}), only the NA-QMD-H approach also reproduces the full quantum results for differential quantities (kinetic-energy spectra $P(E)$ of the particles).

We plan to apply the NA-QMD-H approach first to atom-atom, atom-molecule, and atom-cluster collisions, and we will also elaborate the electronic and vibrational excitation patterns in comparison with existing, still unexplained, experimental data [61] (paper II of this series). Another field of future applications concerns the excited-state relaxation dynamics of photoexcited organic molecules [62] (paper III of this series).

ACKNOWLEDGMENTS

We gratefully acknowledge the allocation of computer resources from the ZIH of the Technische Universität Dresden and the financial support from the Deutsche Forschungsgemeinschaft through the Normalverfahren.

[1] H. Nakamura, *Nonadiabatic Transition: Concepts, Basic Theories and Applications* (World Scientific, Singapore, 2002).
[2] A. Assion, M. Geisler, J. Helbing, V. Seyfried, and T. Baumert, Phys. Rev. A **54**, R4605 (1996).
[3] E. Gagnon, P. Ranitovic, X.-M. Tong, C. L. Cocke, M. M. Murnane, H. C. Kapteyn, and A. S. Sandhu, Science **317**, 1374 (2007).
[4] P. H. Bucksbaum, A. Zavriyev, H. G. Muller, and D. W. Schumacher, Phys. Rev. Lett. **64**, 1883 (1990).
[5] I. Bocharova, R. Karimi, E. F. Penka, J.-P. Brichta, P. Lassonde, X. Fu, J.-C. Kieffer, A. D. Bandrauk, I. Litvinyuk, J. Sanderson, and F. Legare, Phys. Rev. Lett. **107**, 063201 (2011).
[6] C. Horn, M. Wollenhaupt, M. Krug, T. Baumert, R. de Nalda, and L. Bañares, Phys. Rev. A **73**, 031401 (2006).
[7] P. Farmanara, V. Stert, and W. Radloff, Chem. Phys. Lett. **288**, 518 (1998).
[8] M. Lezius, S. Dobosz, D. Normand, and M. Schmidt, Phys. Rev. Lett. **80**, 261 (1998).
[9] A. H. Zewail, Science **242**, 1645 (1988).
[10] J. Opitz, H. Lebius, S. Tomita, B. A. Huber, P. Moretto Capelle, D. Bordenave Montesquieu, A. Bordenave Montesquieu, A. Reinköster, U. Werner, H. O. Lutz, A. Niehaus, M. Benndorf, K. Haghighat, H. T. Schmidt, and H. Cederquist, Phys. Rev. A **62**, 022705 (2000).
[11] J. A. Fayeton, M. Barat, J. C. Brenot, H. Dunet, Y. J. Picard, U. Saalmann, and R. Schmidt, Phys. Rev. A **57**, 1058 (1998).
[12] E. E. B. Campbell and F. Rohmund, Rep. Prog. Phys. **63**, 1061 (2000).
[13] F. Anis and B. D. Esry, Phys. Rev. A **77**, 033416 (2008).
[14] M. Winter, R. Schmidt, and U. Thumm, Phys. Rev. A **80**, 031401 (2009).
[15] X. Guan, K. Bartschat, and B. I. Schneider, Phys. Rev. A **84**, 033403 (2011).
[16] A. S. Simonsen, S. A. Sørngård, R. Nepstad, and M. Førre, Phys. Rev. A **85**, 063404 (2012).
[17] X. Guan, K. Bartschat, B. I. Schneider, and L. Koesterke, Phys. Rev. A **88**, 043402 (2013).
[18] J. L. Sanz-Vicario, H. Bachau, and F. Martín, Phys. Rev. A **73**, 033410 (2006).
[19] G. Sansone, F. Kelkensberg, J. F. Perez-Torres, F. Morales, M. F. Kling, W. Siu, O. Ghafur, P. Johnsson, M. Swoboda, E. Benedetti, F. Ferrari, F. Lepine, J. L. Sanz-Vicario, S. Zherebtsov, I. Znakovskaya, A. L'Huillier, M. Y. Ivanov, M. Nisoli, F. Martin, and M. J. J. Vrakking, Nature (London) **465**, 763 (2010).
[20] J. C. Tully, J. Chem. Phys. **137**, 22A301 (2012).
[21] U. Saalmann and R. Schmidt, Z. Phys. D **38**, 153 (1996).
[22] T. Kunert and R. Schmidt, Eur. Phys. J. D **25**, 15 (2003).
[23] M. A. L. Marques, A. Castro, G. F. Bertsch, and A. Rubio, Comput. Phys. Commun. **151**, 60 (2003).
[24] P.-G. Reinhard and E. Suraud, J. Cluster Sci. **10**, 239 (1999).
[25] A. Anderson, Phys. Rev. Lett. **74**, 621 (1995).
[26] J. Caro and L. L. Salcedo, Phys. Rev. A **60**, 842 (1999).
[27] O. V. Prezhdo and P. J. Rossky, J. Chem. Phys. **107**, 825 (1997).
[28] U. Saalmann and R. Schmidt, Phys. Rev. Lett. **80**, 3213 (1998).
[29] T. Kunert and R. Schmidt, Phys. Rev. Lett. **86**, 5258 (2001).
[30] T. Laarmann, I. Shchatsinin, A. Stalmashonak, M. Boyle, N. Zhavoronkov, J. Handt, R. Schmidt, C. P. Schulz, and I. V. Hertel, Phys. Rev. Lett. **98**, 058302 (2007).
[31] W. Domcke and G. Stock, in *Advances in Chemical Physics* (Wiley, Hoboken, NJ, 2007), pp. 1–169.
[32] O. Butriy, H. Ebadi, P. L. de Boeij, R. van Leeuwen, and E. K. U. Gross, Phys. Rev. A **76**, 052514 (2007).
[33] M. Ben-Nun and T. J. Martinez, Chem. Phys. Lett. **298**, 57 (1998).
[34] A. P. Horsfield, D. R. Bowler, A. J. Fisher, T. N. Todorov, and C. G. Sánchez, J. Phys. Condens. Matter **16**, 8251 (2004).
[35] F. Grossmann, U. Saalmann, and R. Schmidt, Ann. Phys. (Berlin, Ger.) **9**, 785 (2000).
[36] N. L. Doltsinis and D. Marx, Phys. Rev. Lett. **88**, 166402 (2002).
[37] C. F. Craig, W. R. Duncan, and O. V. Prezhdo, Phys. Rev. Lett. **95**, 163001 (2005).
[38] E. Tapavicza, I. Tavernelli, and U. Rothlisberger, Phys. Rev. Lett. **98**, 023001 (2007).
[39] E. Runge and E. K. U. Gross, Phys. Rev. Lett. **52**, 997 (1984).
[40] J. C. Tully, J. Chem. Phys. **93**, 1061 (1990).
[41] M. Uhlmann, T. Kunert, and R. Schmidt, J. Phys. B **39**, 2989 (2006).
[42] M. Uhlmann, T. Kunert, and R. Schmidt, Phys. Rev. E **72**, 036704 (2005).
[43] http://www.dymol.org/.

[44] Z. Roller-Lutz, Y. Wang, H. O. Lutz, U. Saalmann, and R. Schmidt, Phys. Rev. A **59**, R2555 (1999).
[45] O. Knospe, J. Jellinek, U. Saalmann, and R. Schmidt, Eur. Phys. J. D **5**, 1 (1999).
[46] O. Knospe, J. Jellinek, U. Saalmann, and R. Schmidt, Phys. Rev. A **61**, 022715 (2000).
[47] M. Ehrich, U. Werner, H. O. Lutz, T. Kaneyasu, K. Ishii, K. Okuno, and U. Saalmann, Phys. Rev. A **65**, 030702 (2002).
[48] R. Schmidt and J. Handt, in *Laser- and Collision-Induced Collective Vibrational Excitations in Fullerenes*, edited by A. Solovyov and E. Surdutovich AIP Conf. Proc. 1197 (AIP, New York, 2009), pp. 144–151.
[49] T. Kunert, F. Grossmann, and R. Schmidt, Phys. Rev. A **72**, 023422 (2005).
[50] J. Handt, T. Kunert, and R. Schmidt, Chem. Phys. Lett. **428**, 220 (2006).
[51] M. Fischer, J. Handt, G. Seifert, and R. Schmidt, Phys. Rev. A **88**, 061403 (2013).
[52] M. Uhlmann, T. Kunert, F. Grossmann, and R. Schmidt, Phys. Rev. A **67**, 013413 (2003).
[53] M. Uhlmann, T. Kunert, and R. Schmidt, Phys. Rev. A **72**, 045402 (2005).
[54] M. Fischer, J. Handt, J.-M. Rost, F. Grossmann, and R. Schmidt, Phys. Rev. A **86**, 053821 (2012).
[55] Extensible computational chemistry environment basis set database, https://bse.pnl.gov/bse/portal.
[56] D. Feller, J. Comput. Chem. **17**, 1571 (1996).
[57] K. L. Schuchardt, B. T. Didier, T. Elsethagen, L. Sun, V. Gurumoorthi, J. Chase, J. Li, and T. L. Windus, J. Chem. Inf. Model. **47**, 1045 (2007).
[58] O. Knospe, R. Schmidt, and G. Seifert, in *Advances in Classical Trajectory Methods*, edited by W. L. Hase, Molecular Dynamics of Clusters, Surfaces, Liquids, and Interfaces Vol. 4 (JAI Press, Stamford, Connecticut, 1999), p. 153.
[59] F. Rohmund, E. E. B. Campbell, O. Knospe, G. Seifert, and R. Schmidt, Phys. Rev. Lett. **76**, 3289 (1996).
[60] G. P. Zhang and T. F. George, Phys. Rev. Lett. **93**, 147401 (2004).
[61] M. Fischer, J. Handt, and R. Schmidt, Paper II of this series, Phys. Rev. A **90**, 012526 (2014).
[62] M. Fischer, J. Handt, and R. Schmidt, Paper III of this series, Phys. Rev. A **90**, 012527 (2014).
[63] The scalar product denotes integration over the electronic coordinates and summation over the electronic spins.
[64] A. Zangwill and P. Soven, Phys. Rev. Lett. **45**, 204 (1980).
[65] A. Zangwill and P. Soven, Phys. Rev. B **24**, 4121 (1981).
[66] T. Kunert, Ph.D. thesis, Technische Universität Dresden, 2003.
[67] A. Görling, Phys. Rev. A, **54**, 3912 (1996).
[68] S. A. Fischer, B. F. Habenicht, A. B. Madrid, W. R. Duncan, and O. V. Prezhdo, J. Chem. Phys. **134**, 024102 (2011).
[69] L. F. Errea, L. Fernandez, A. Macias, L. Mendez, I. Rabadan, and A. Riera, J. Chem. Phys. **121**, 1663 (2004).
[70] M. Fischer, U. Lorenz, B. Schmidt, and R. Schmidt, Phys. Rev. A **84**, 033422 (2011).
[71] I. Tavernelli, B. F. E. Curchod, and U. Rothlisberger, Phys. Rev. A **81**, 052508 (2010).
[72] F. T. Smith, Phys. Rev. **179**, 111 (1969).
[73] B. Schmidt and U. Lorenz, WAVEPACKET 4.7, http://wavepacket.sourceforge.net.
[74] M. R. Hermann and J. A. Fleck, Jr., Phys. Rev. A **38**, 6000 (1988).
[75] U. Saalmann, Ph.D. thesis, Technische Universität Dresden, 1997.